CR 73067

ME-661

HEAT TRANSFER CHARACTERISTICS OF ARC TUNNEL CONSTRICTORS

Prepared under Contract NAS2-2640
For NASA-Ames Research Center

by

Darryl E. Metzger

HEAT TRANSFER CHARACTERISTICS OF ARC TUNNEL CONSTRICTORS

Report No. ME-661

Prepared under Contract NAS2-2640

for

National Aeronautics and Space Administration
Ames Research Center

by

Darryl E. Metzger

Engineering Research Center
ARIZONA STATE UNIVERSITY
Tempe, Arizona

August 15, 1966

ABSTRACT

Arc tunnel constrictors have been designed and tested which will tolerate heat fluxes up to 12,000 Btu/(sec ft^2). Thick walled constrictors failed by local melting on the arc side of the wall at flux levels in agreement with predictions based on axisymmetric conduction through the wall. Burnout type failures were observed with thinner walled constrictors at flux levels up to four times higher than predicted by Gambill's additive method, and the difference is attributed to high non-boiling convective heat transfer rates. The results of this study indicate that with proper coolant passage design and high coolant pressures, heat fluxes up to 20,000 Btu/(sec ft^2) may be tolerable without constrictor failure.

TABLE OF CONTENTS

LIST OF FIGURES

REFERENCES

1. "The Theoretical Enthalpy Distribution of Air in Steady Flow Along the Axis of a Direct-Current Electric Arc", by H. A. Stine and V. R. Watson, NASA TN D-1331, 1962.
2. "Evaluation of a Constricted-Arc Supersonic Jet", by C. E. Shepard, V. R. Watson, and H. A. Stine, NASA TN D-2066, 1964.
3. "Heat Transfer in Tube Coils With Laminar and Turbulent Flow", by R. A. Seban and E. F. McLaughlin, International Journal of Heat and Mass Transfer, Vol. 6, pp. 387-395, 1963.
4. "Subcooled Boiling Heat Transfer Under Forced Convection in a Heated Tube", by S. S. Papell, NASA TN D-1583, 1963.
5. "Generalized Prediction of Burnout Heat Flux for Flowing, Subcooled, Wetting Liquids", by W. R. Gambill, Chemical Engineering Progress Symposium Series, Volume 59, No. 41, 1963.
6. "Correlation of Maximum Heat Transfer Data for Boiling of Saturated Liquids", by W. Rohsenow and P. Griffith, Chemical Engineering Progress Symposium Series, Vol. 52, No. 18, 1956.
7. Nuclear Engineering, pp. 399-431, McGraw-Hill, New York, 1957.
8. "A Theory of Local Boiling Burnout and Its Application to Existing Data", by L. Bernath, Chemical Engineering Progress Symposium Series, Vol. 56, No. 30, 1960.
9. "Subcooled Burnout in Tubes of Small Diameter", by A. E. Bergles, ASME Paper No. 63-WA-182, November, 1963.

NOMENCLATURE

English Letter Symbols

c_p	coolant specific heat, Btu/(lbm ^oF)
D_h	hydraulic diameter, ft
h	heat transfer coefficient, Btu/(hr ft^2 ^oF)
k	thermal conductivity of constrictor disk, Btu/(hr ft ^oF)
$\dot{q}/A$	heat flux, Btu/(hr ft^2) or Btu/(sec ft^2)
r	radius of coolant passage wall, ft
T,t	temperature, ^oF
V	mean velocity, ft/hr or ft/sec
v	specific volume, ft^3/lbm

Greek Letter Symbols

α	thermal diffusivity of coolant, ft^2/hr
μ	viscosity, lbm/(ft hr)
ρ	density, lbm/ft^3

Non-Dimensional Quantities

F_{sub}	subcooling factor, defined by Equation 10
Pr	Prandtl Number, $\mu/(\rho\alpha)$
Re	Reynolds Number, $V\rho D_h/\mu$
St	Stanton Number, $h/(V\rho c_p)$

Subscripts

av	denotes average
b	denotes bulk average
f	indicates a property at saturated liquid condition
g	indicates a property at saturated vapor condition
i	indicates a variable either evaluated at the inner coolant wall radius or at the coolant passage inlet conditions
o	indicates a variable either evaluated at the outer coolant wall radius or at the coolant passage discharge conditions
w	indicates a variable evaluated at the coolant passage wall

I. Introduction

The constricted arc wind tunnel is a research facility currently in use wherever steady flows of high enthalpy are required. Such devices are used, for example, to study ablation and heat transfer characteristics of space vehicles upon entry into various planetary atmospheres. NASA's Ames Research Center has been involved both in the development of the constricted arc tunnels and in their use as a research tool. The present report, dealing with performance characteristics of arc tunnels, covers work carried out by the Engineering Research Center at Arizona State University under NASA-Ames Research Center sponsorship.

A schematic of a constricted arc tunnel is shown in Fig. 1. Basically, the device consists of an anode and cathode separated by a segmented, cooled nozzle. In operation, the test gas is injected near the cathode and accelerated through the nozzle into the test section of the tunnel. The ionized test gas carries a high d.c. current between the cathode and the anode; in effect the arc is carried through the nozzle, heating the test gas to high enthalpy levels in the process.

A considerable portion of the electrical power dissipated in the plasma is lost to the constrictor walls through heat transfer. The operation of the device is such that increases in energy content of the test gas are necessarily accompanied by increases in constrictor wall heat transfer. As a consequence, the ultimate performance of these devices is limited by the maximum tolerable wall heat flux.

For steady state operation, the wall heating from the plasma must be removed by the coolant. The basic constrictor configuration is shown in Fig. 2, and consists of a thin disk with a circular plasma passage and an annular coolant passage. The disk material usually employed is copper and the coolant is usually water. The capability of the coolant for removing the wall heating is enhanced by allowing the coolant to boil; however, the crisis point associated with the transition from nucleate to pool boiling suggests that constricted arc performance will be limited to coolant heat fluxes lower than this transition value.

The present study deals with the heat removal capabilities of cooled constricted disks; further discussion of the theory of constricted arc jets may be found in References 1 and 2.

FIGURE 1
SCHEMATIC OF A CONSTRICTED ARC

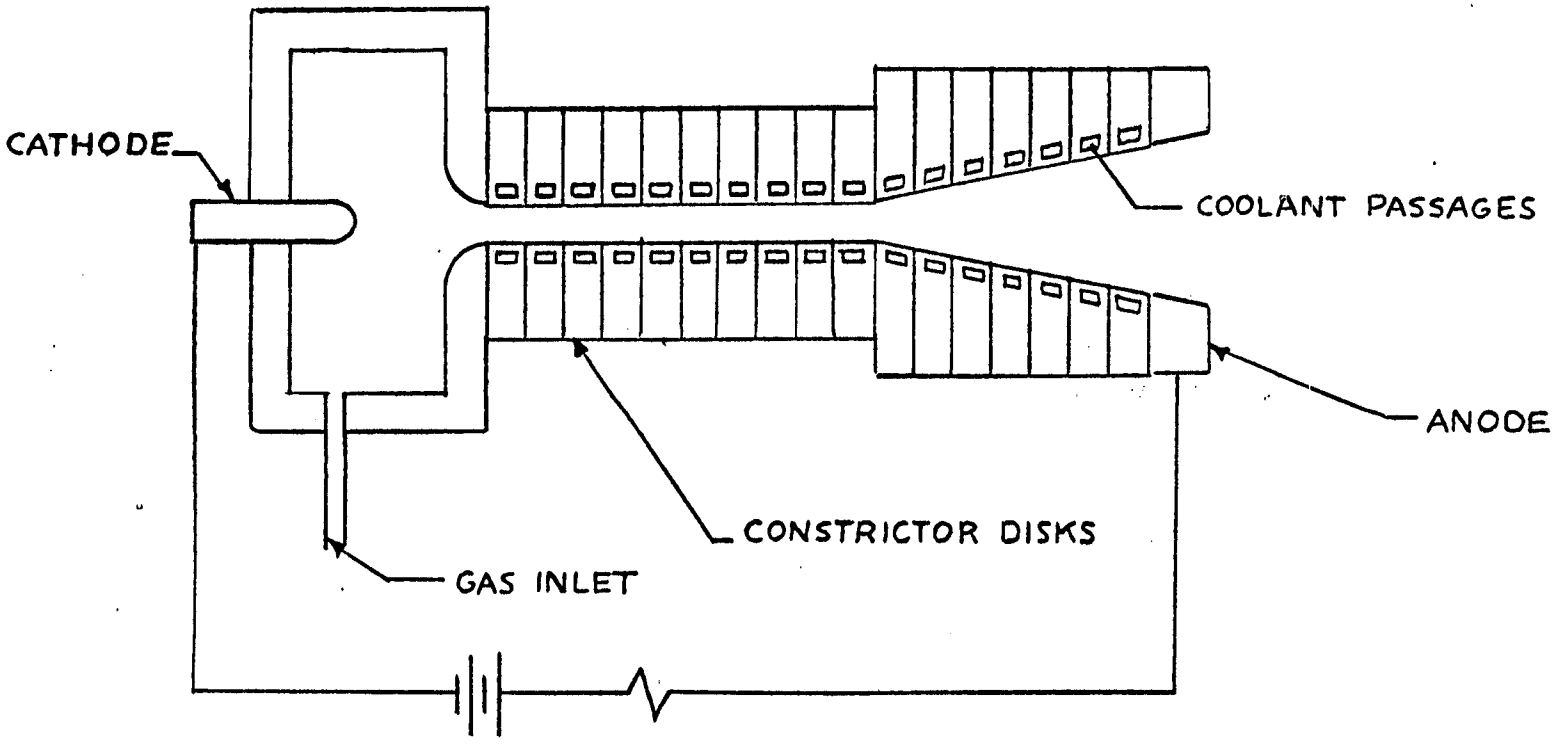

II. Basic Considerations of the Heat Transfer Problem

The constrictor geometry under consideration may be idealized as follows. A plasma passage of circular cross section is separated from a concentric cooling passage by a copper annulus as shown in Fig. 2. Assuming one-dimensional axi-symmetrical radial conduction, the temperature drop through the copper wall and the heat fluxes at the inner and outer radii are related through the steady state conduction rate equation:

$$\frac{\dot{q}}{A_i} = \frac{T_i - T_o}{\ln(r_o/r_i)} \cdot \frac{k}{r_i} \qquad \text{- - - - - - - - - - (1)}$$

$$\frac{\dot{q}}{A_o} = \frac{T_i - T_o}{\ln(r_o/r_i)} \cdot \frac{k}{r_o}$$

For a given plasma passage diameter, the inner and outer heat fluxes can be evaluated from Equation 1 as a function of the wall temperature drop and radius ratio, r_o/r_i, as shown in Fig. 3 for a 1/4" diameter copper constrictor.

The inner temperature, T_i, cannot exceed the wall material melting point, which for copper is approximately 1980°F. The wall temperature on the coolant side, T_o, will vary depending on the coolant, coolant pressure, flow conditions, and whether or not surface boiling is occurring. Nevertheless, for the flux levels under consideration, T_o will rarely either exceed 450°F or be less than 250°F. Thus the maximum possible non-melting wall temperature difference may be represented as a band centering at 1650°F as shown in Fig. 3.

The coolant wall temperatures quoted above are valid only in the non-boiling and nucleate boiling coolant regimes. At some value of the coolant flux, $(\dot{q}/A_o)$, nucleate boiling cannot be maintained, and as a transition to the film boiling regime occurs, with a concurrent rapid rise in T_o, T_i also rapidly rises past the melting point, thus the critical heat flux must be considered as a limit, beyond which the constrictor cannot operate. An often quoted, though seldom achieved, limiting value of the critical heat flux is 10,000 Btu/sec.ft.^{2}, and this value is also indicated in Fig. 3.

From Fig. 3, it can be seen that two modes of constrictor failure are possible. Failure may be due to a transition to film boiling; alternatively, the large gradients set up in a relatively thick wall may cause melting at flux levels well below the critical level.

Figs. 4 and 5 show similar plots of equations 1 for 1/2" and 1" diameter constrictors.

FIGURE 2

CONSTRICTOR GEOMETRY AND NOMENCLATURE

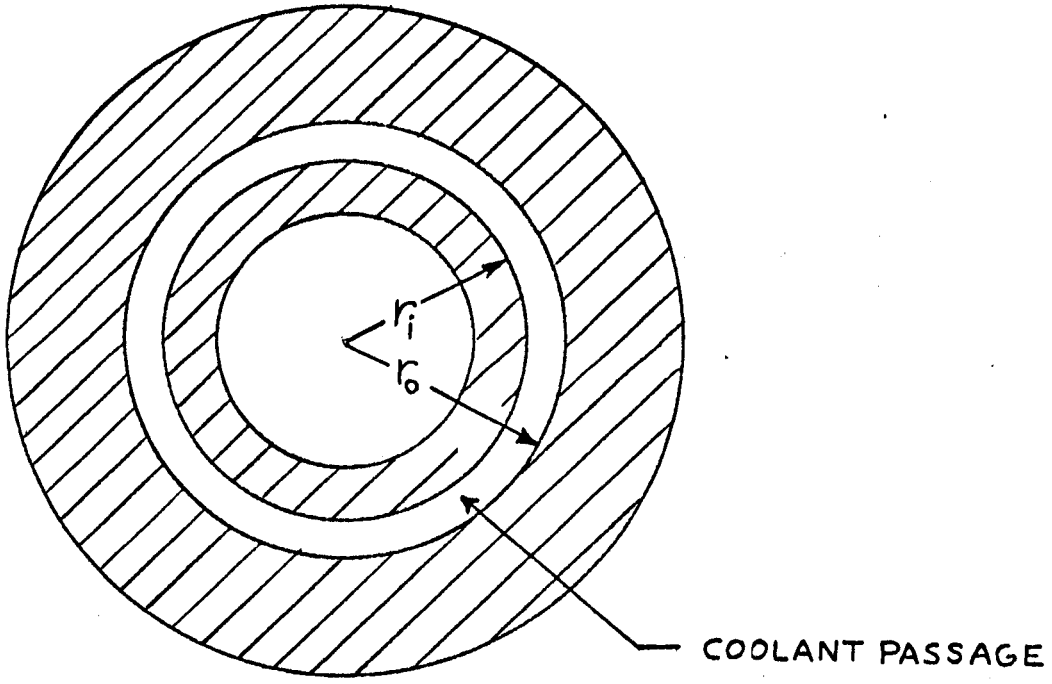

FIGURE 3
CONDUCTION THROUGH $\frac{1}{4}$" D CONSTRICTORS

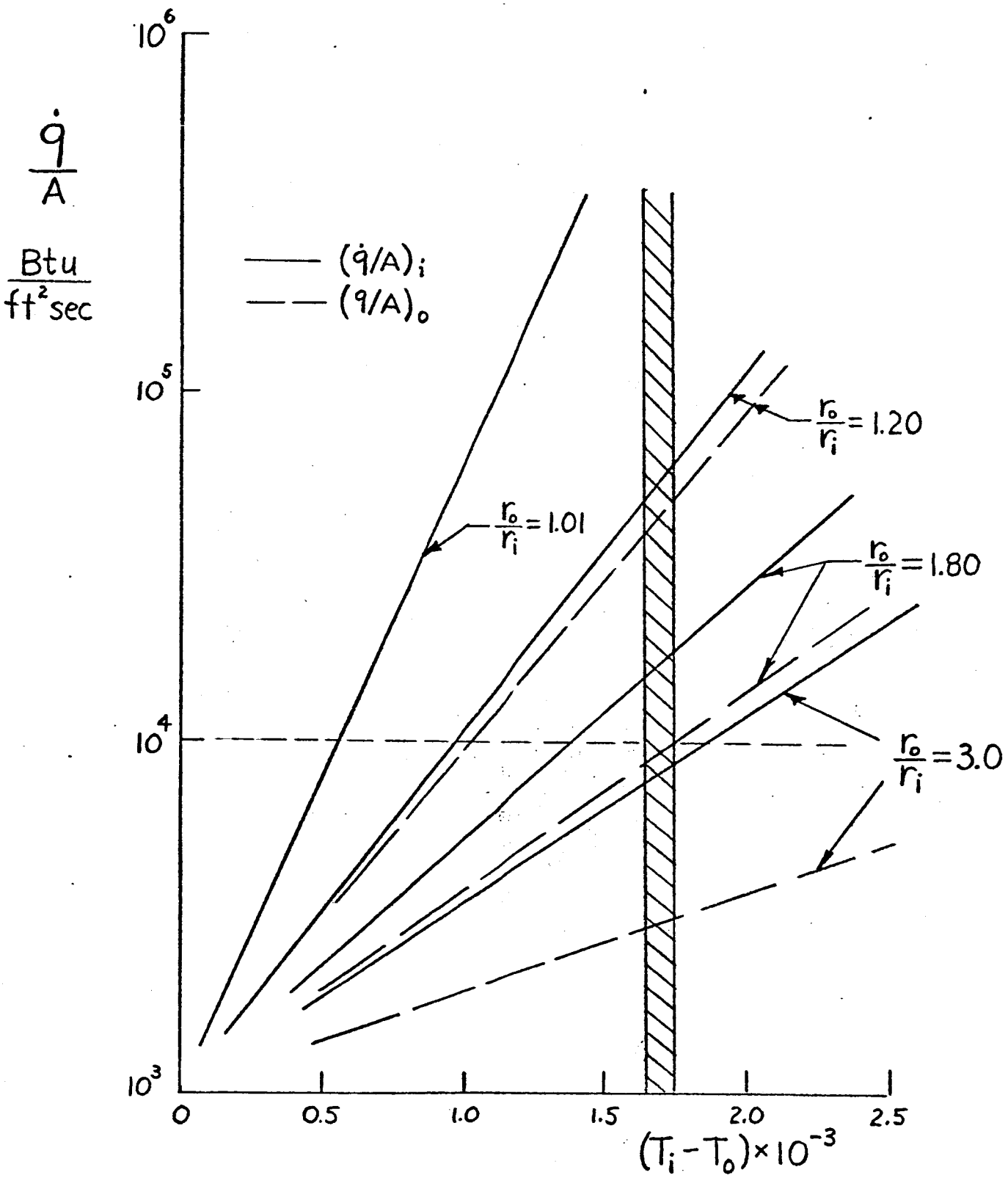

FIGURE 4
CONDUCTION THROUGH $\frac{1}{2}$" D CONSTRICTORS

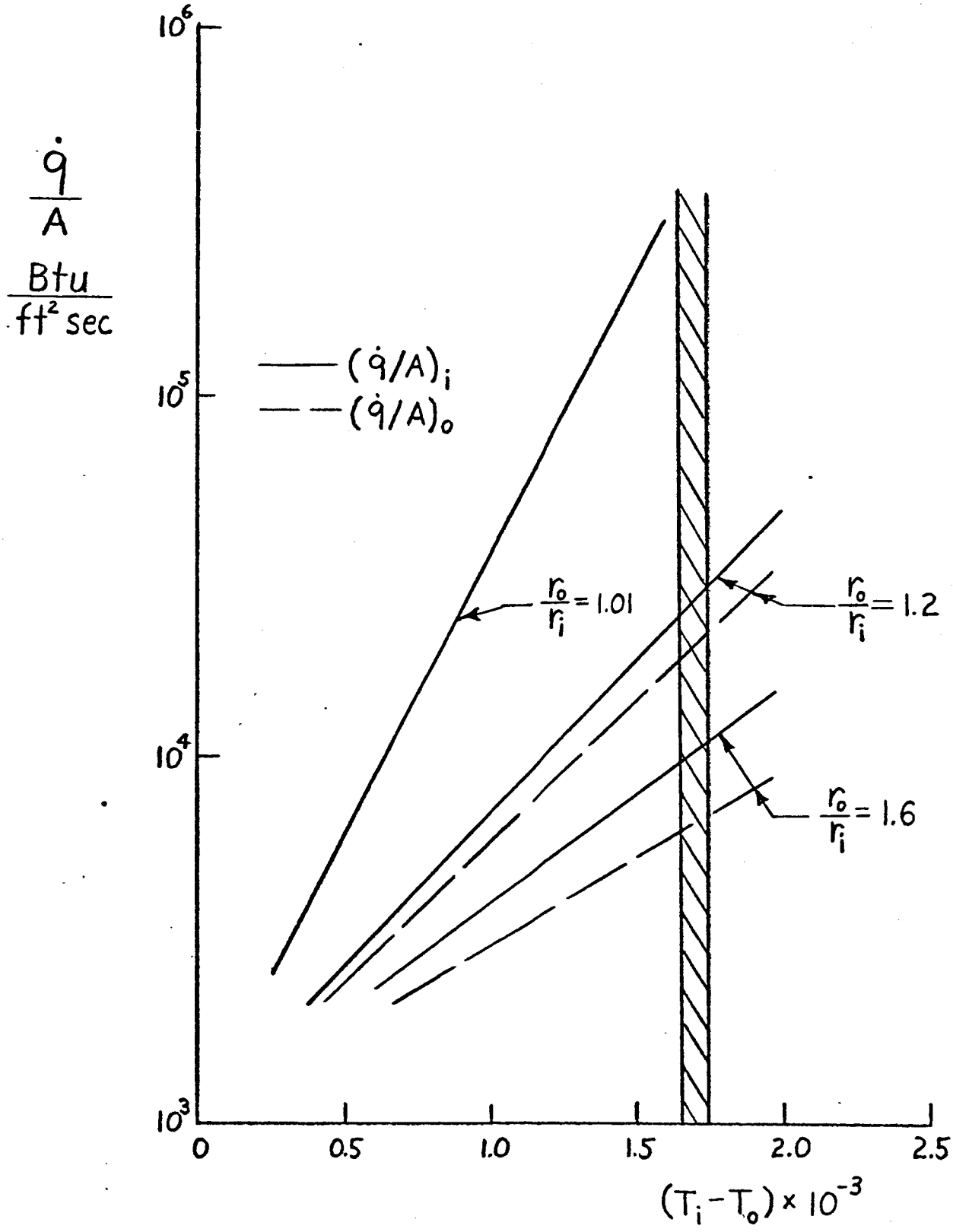

FIGURE 5
CONDUCTION THROUGH 1"D CONSTRICTORS

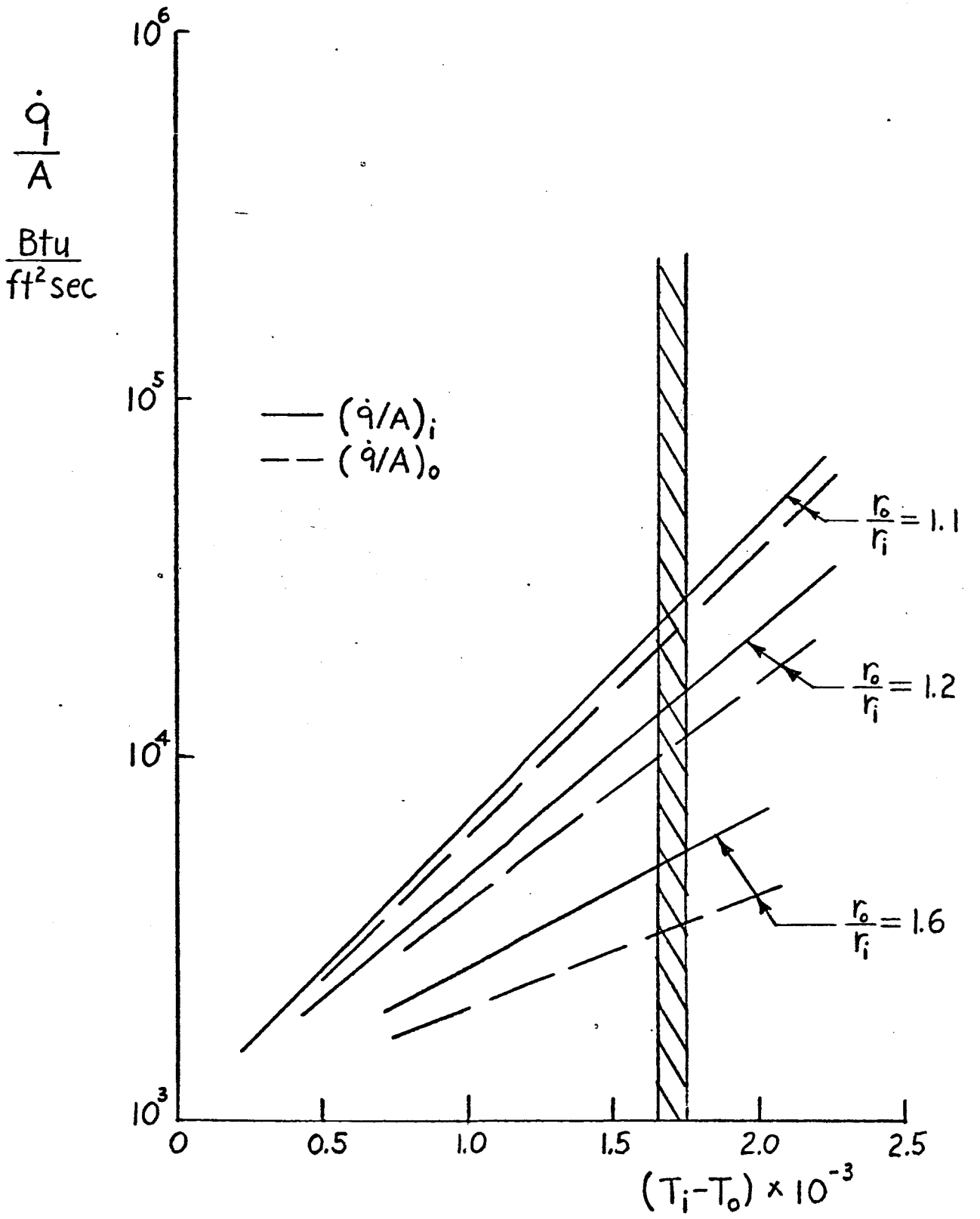

III. Performance Possibilities of Non-Boiling Convective Cooling

Seban and McLaughlin (Reference 3) report heat transfer coefficients obtained from experiments with turbulent flow in curved passages, the general configuration of the constrictor coolant passages. Data is reported only for passages of circular cross section and uniform peripheral heating; whereas the constrictors have rectangular passages with the heating concentrated at one side. They found that the average peripheral heat transfer coefficients exceeded those for straight tubes. Expressed emperically:

$$\frac{h_{curved}}{h_{straight}} = 1 + 3.5\ (d/D) \qquad \text{- - - - - - - - - - (2)}$$

where d is the tube cross section diameter and D is twice the radius of curvature of the tube.

Seban and McLaughlin also measured the difference between the heat transfer coefficients on the inside and outside of the tube curvature. They found that the secondary flow induced in the curved passage significantly lowered the coefficients on the inside. (For d/D = 0.0096 and d/D = 0.059, the inside coefficients were respectively 0.75 and 0.5 of the mean peripheral values.)

In some of the 1/4" diameter constrictors, the coolant passages have d/D ratios of 0.2 and greater, so secondary flow may be expected to have a significant effect on the constrictor heat transfer coefficients. A qualitative picture of the secondary flow pattern is shown in Fig. 6. For the case where heating is at one side of the passage only, it can be seen that the heated wall is continually flushed with fluid from the unheated sides, and the heat transfer rates may be considerably enhanced over the uniform peripheral heating case.

In view of the lack of information available on heat transfer coefficients for the constrictor geometry, the estimation of the performance possibilities of the non-boiling cooling must be considered a rough estimate at best.

For estimation purposes, the heat transfer in the coolant passages will be predicted from the Colburn Equation:

$$St = \frac{h}{\rho v_{cp}} = 0.023\ Pr^{-2/3}\ Re^{-0.2} \qquad \text{- - - - - - - - - - (3)}$$

The heat flux per unit area is given by:

$$\frac{\dot{q}}{A} = h\,(t_w - t_{b,av}) \qquad \text{- - - - - - - - - (4)}$$

where

$$t_{b,av} = (t_{b,i} + t_{b,o})\,/2 \qquad \text{- - - - - - - - - (5)}$$

The maximum possible non-boiling heat transfer rate is attained with the wall temperature at the point of incipient nucleate boiling. The wall temperature at this point has been shown to be of the order of $20^{\circ}F$ of superheat (Reference 4). Thus:

$$t_w = t_{s,o} + 20 \qquad \text{- - - - - - - - - (6)}$$

Note that the bulk temperature rise in the coolant passage is related to the heat flux:

$$\dot{q} = \dot{m}\, c_p\, (t_{b,o} - t_{b,i}) \qquad \text{- - - - - - - - - (7)}$$

For a given passage cross section, flow velocity, and outlet pressure, equations 3 - 7 can be solved iteratively to yield the heat flux at incipient boiling.

Generally, the flow velocity and outlet pressure is related through the total head capability of the system. If we consider the upstream pressure a constant, as dictated by the pressure capabilities of the fittings, etc., then an increase in exit pressure obtained by downstream throttling will be accompanied by a decrease in flow velocity. Experience shows that in the constrictors only about one-half the pressure head difference is converted into kinetic energy, frictional losses accounting for the remainder.

With these assumptions, equations 3 - 7 have been solved for one passage cross section (D_h = 0.09 in.), one bulk inlet temperature ($70^{\circ}F$), and three supply pressures (P_i = 1000, 500, 100) with various outlet pressures. The results are shown in Fig. 7. An increase in outlet pressure at a given supply pressure results in a decrease in flow velocity and an increase in wall temperature, the latter tending to increase the heat transfer and the former tending to decrease it. The result is an optimum outlet pressure for each supply pressure; however, the curves are rather flat near their maximum point.

FIGURE 6
SECONDARY FLOW PATTERNS

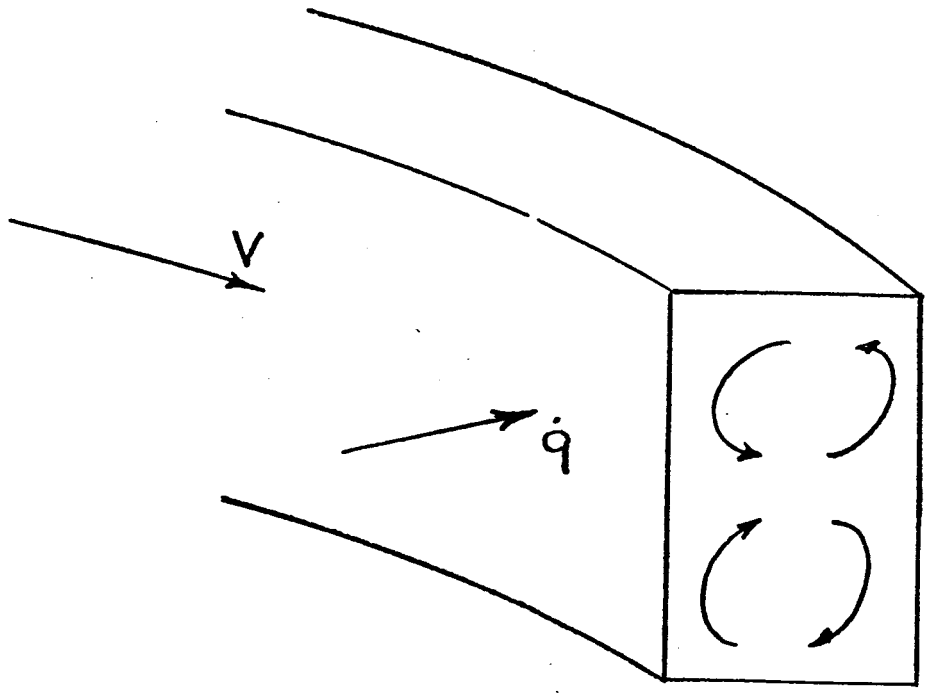

FIGURE 7
NON-BOILING PERFORMANCE

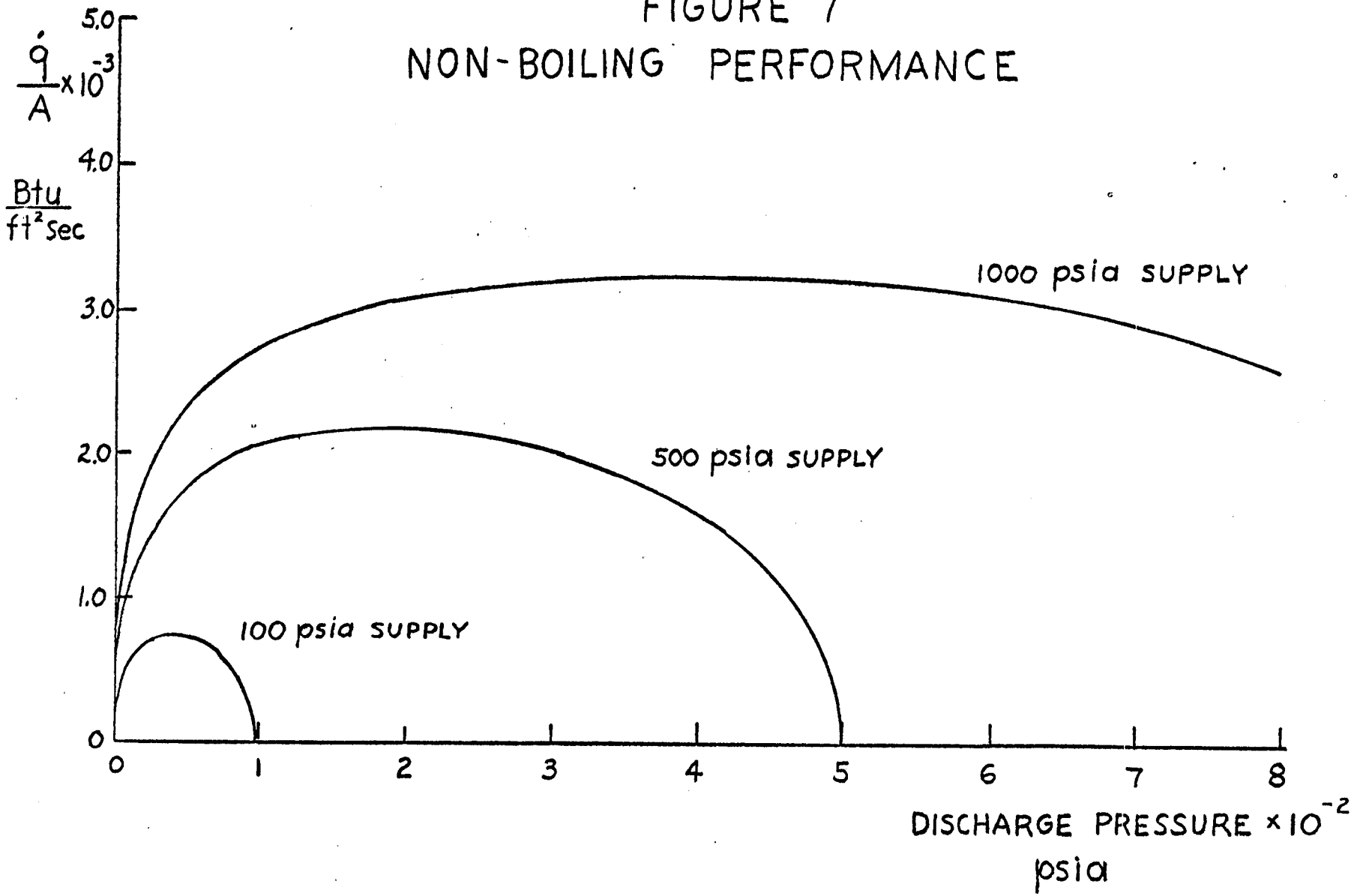

IV. Performance Possibilities with Surface Boiling

The most workable scheme at present for predicting the burnout heat flux in a flow boiling situation is the superposition method where a pool boiling burnout heat flux is added to a forced convection, non-boiling heat flux. The particular scheme which has been most extensively compared with available experimental data is that proposed by Gambill (Reference 5). This scheme predicts the burnout heat flux, $(\dot{q}/A)_{b.o.}$ as:

$$\left(\frac{\dot{q}}{A}\right)_{b.o.} = \left(\frac{\dot{q}}{A}\right)_{Sat\text{-}pool,b.o.} \cdot F_{sub} + \left(\frac{\dot{q}}{A}\right)_{non\text{-}boil,b.o.} \qquad \text{- - - - - (8)}$$

where $(\dot{q}/A)_{Sat\text{-}pool,b.o.} \cdot F_{sub}$ represents the boiling contribution to the burnout heat flux in the absence of forced convection and $(\dot{q}/A)_{non\text{-}boil,b.o.}$ represents the forced convection contribution in the absence of boiling. The term $(\dot{q}/A)_{Sat\text{-}pool,b.o.}$ represents saturated pool boiling burnout and F_{sub} is a factor introduced to correct the saturated pool boiling burnout results for non-saturated, or subcooled, conditions.

The available experimental evidence indicates that many of the available correlations for $(\dot{q}/A)_{Sat\text{-}pool,b.o.}$ can be used with success in this superposition method. For simplicity, the Rohsenow-Griffith equation (Reference 6) has been used in the present study.

$$\left(\frac{\dot{q}}{A}\right)_{Sat\text{-}pool,b.o.} = 143\, h_{fg} \left(\frac{1}{v_g}\right) \left[\frac{v_g}{v_f} - 1\right]^{0.6} \qquad \text{- - - - - (9)}$$

The ratio of the subcooled to saturated pool-boiling burnout heat flux, F_{sub}, is given by Bonilla (Reference 7).

$$F_{sub} = 1 + \frac{c_p\, \Delta t_{sub}}{25\, h_{fg}} \left(\frac{v_g}{v_f}\right)^{0.923} \qquad \text{- - - - - (10)}$$

The non-boiling contribution at burnout is calculated from the convective rate equation:

$$\left(\frac{\dot{q}}{A}\right)_{non\text{-}boil,b.o.} = h\, (t_w - t_{b,av})_{b.o.} \qquad \text{- - - - - (11)}$$

The calculation of this latter contribution requires knowledge of the amount of wall superheat at burnout; however, considerable disagreement exists in the published literature as to this amount. Bernath (Reference 8) has given a general relation for the amount of wall superheat (at burnout) which indicates reductions in wall superheat with increases in flow velocity. Because of the evident uncertainty in the exact level of wall superheat at burnout, the convective contribution to the burnout heat flux has been calculated with wall temperatures of 20°F above saturation. This is approximately the amount of superheat at incipient boiling, and should result in a somewhat conservative estimate of the burnout heat flux.

The non-boiling contribution, $(\dot{q}/A)_{non\text{-}boil,b.o.}$, is thus given for the present system by Figure 7. The saturated pool boiling contribution and subcooling factor have been evaluated for a bulk temperature of 70°F for a range of pressures up to the critical pressure, and these are presented in Figures 8 and 9. The total non-convective contribution, $(\dot{q}/A)_{Sat\text{-}pool,b.o.} \cdot F_{sub}$ is plotted in Figure 10. It should be noted that one apparent effect of large amounts of subcooling is to lower the optimum pressure for maximum heat flux far below the one-third critical pressure generally recognized for saturated boiling and evident in Figure 8.

Finally, if the boiling and convective contribution of Figures 7 and 10 are summed, the predicted burnout flux as a function of supply and discharge pressures is as shown in Figure 11. These results indicate that for maximum heat fluxes, the passage outlet pressure should be maintained at from one-third to one-half the supply pressure.

Most of the available experimental data for subcooled flow boiling has been obtained with passage hydraulic diameters much larger than those required for the constrictor cooling. One notable exception to this is the work of Bergles (Reference 9). He presents burnout data for straight circular tubes with diameters and lengths comparable to those employed in the constrictors.

The superposition scheme outlined above has been used to predict the effect of outlet pressure on burnout flux for the condition presented in Figure 3 of Reference 9. This comparison is shown in Figure 12, and indicates the predicted values are approximately 50% of the observed values. Nevertheless, the observed trend of the results with outlet pressure is similar to that predicted, and the

difference in magnitude can perhaps be explained by the inadequacy of Equation 3 and the conservative estimate of the wall superheat at burnout. This comparison lends some degree of confidence to the use of the superposition scheme for predicting the effect of coolant pressure on the burnout flux.

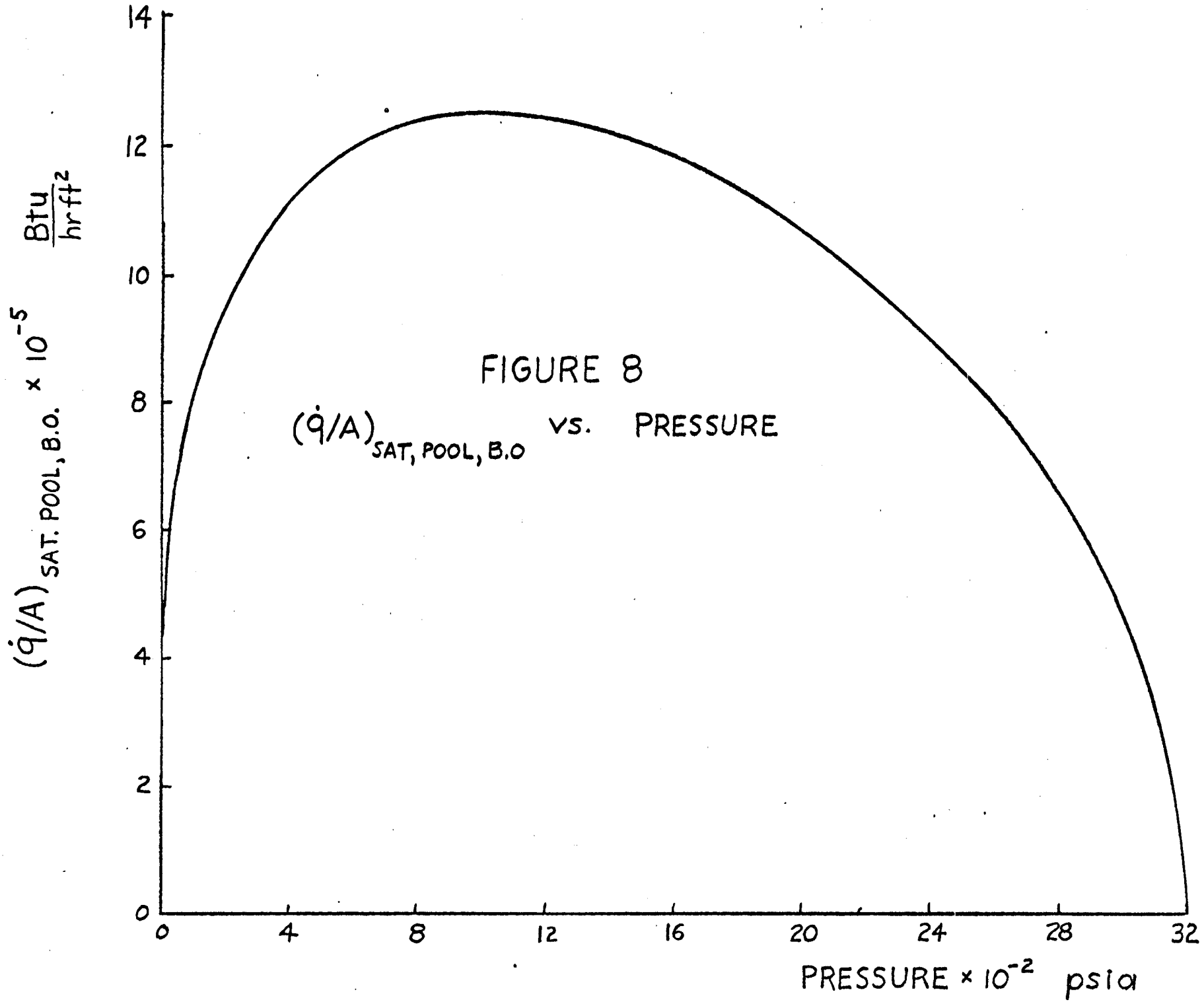

FIGURE 8

$(\dot{q}/A)_{SAT, POOL, B.O}$ vs. PRESSURE

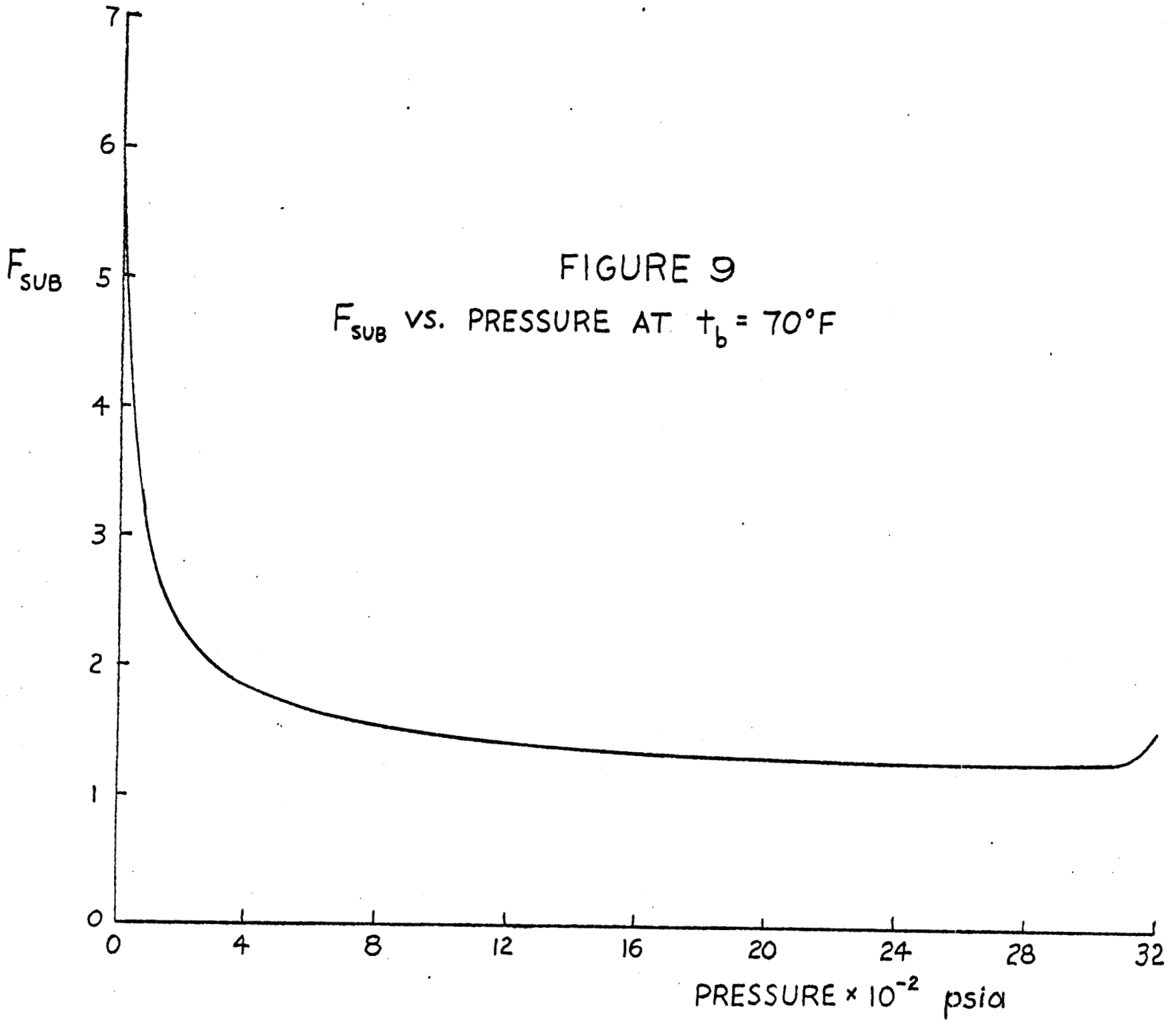
FIGURE 9
F_{SUB} VS. PRESSURE AT t_b = 70°F
F_{SUB}
7
6
5
4
3
2
1
0
0
4
8
12
16
20
24
28
32
PRESSURE × 10^{-2} psia

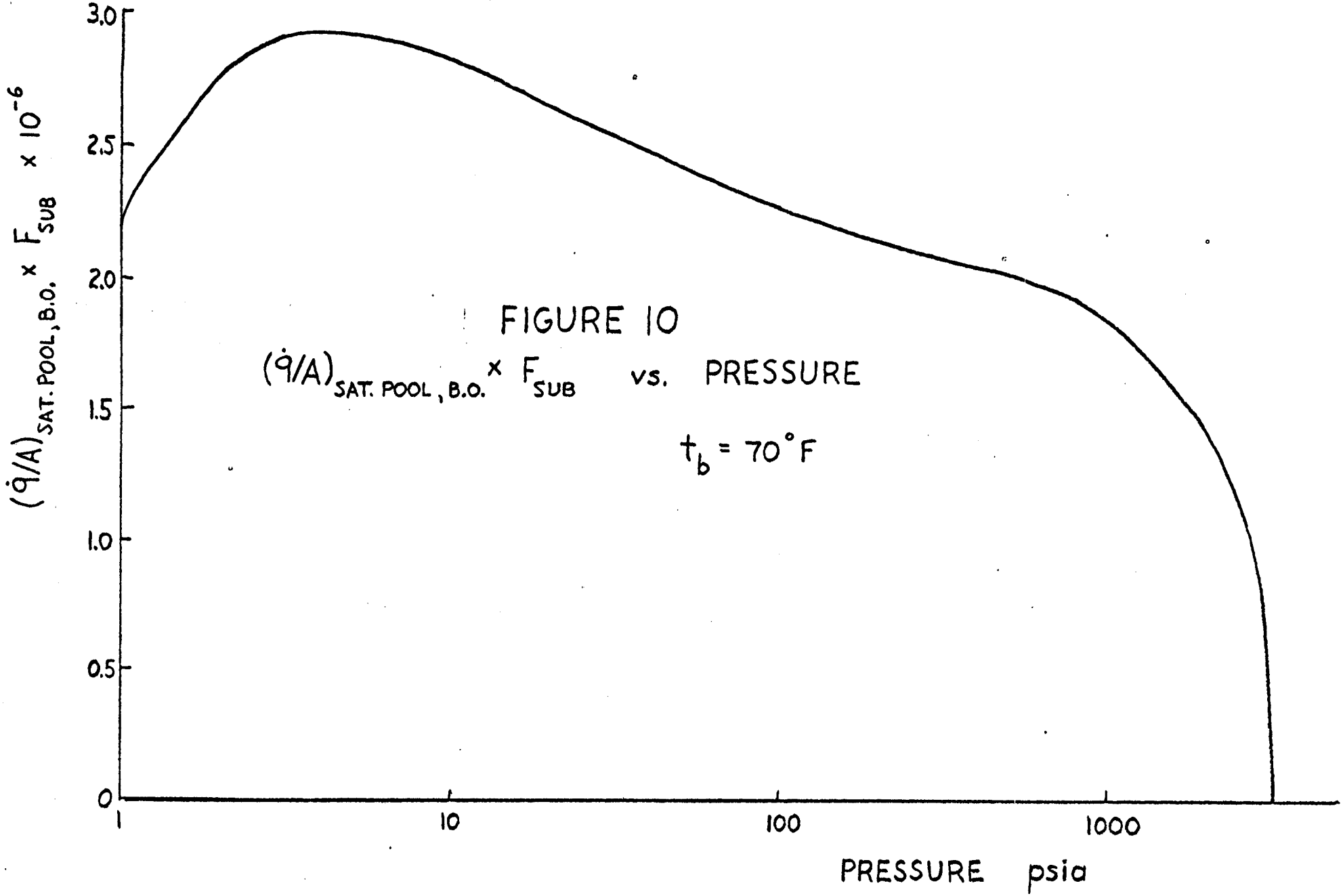

FIGURE 10

$(\dot{q}/A)_{SAT.\ POOL,\ B.O.} \times F_{SUB}$ vs. PRESSURE

$t_b = 70°F$

FIGURE 11

BOILING PERFORMANCE

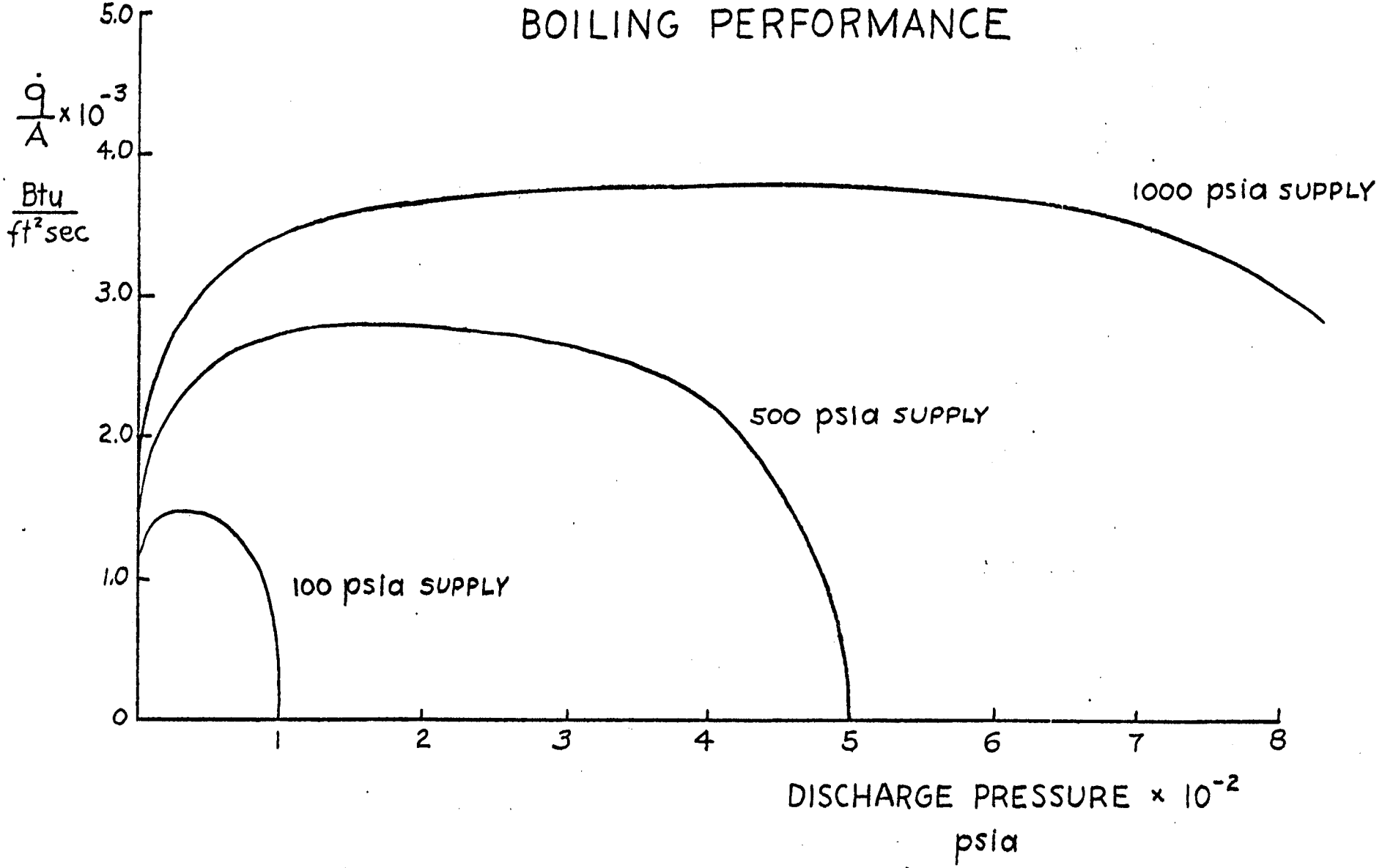

FIGURE 12

COMPARISON – DATA OF REF. 9 AND PREDICTIONS

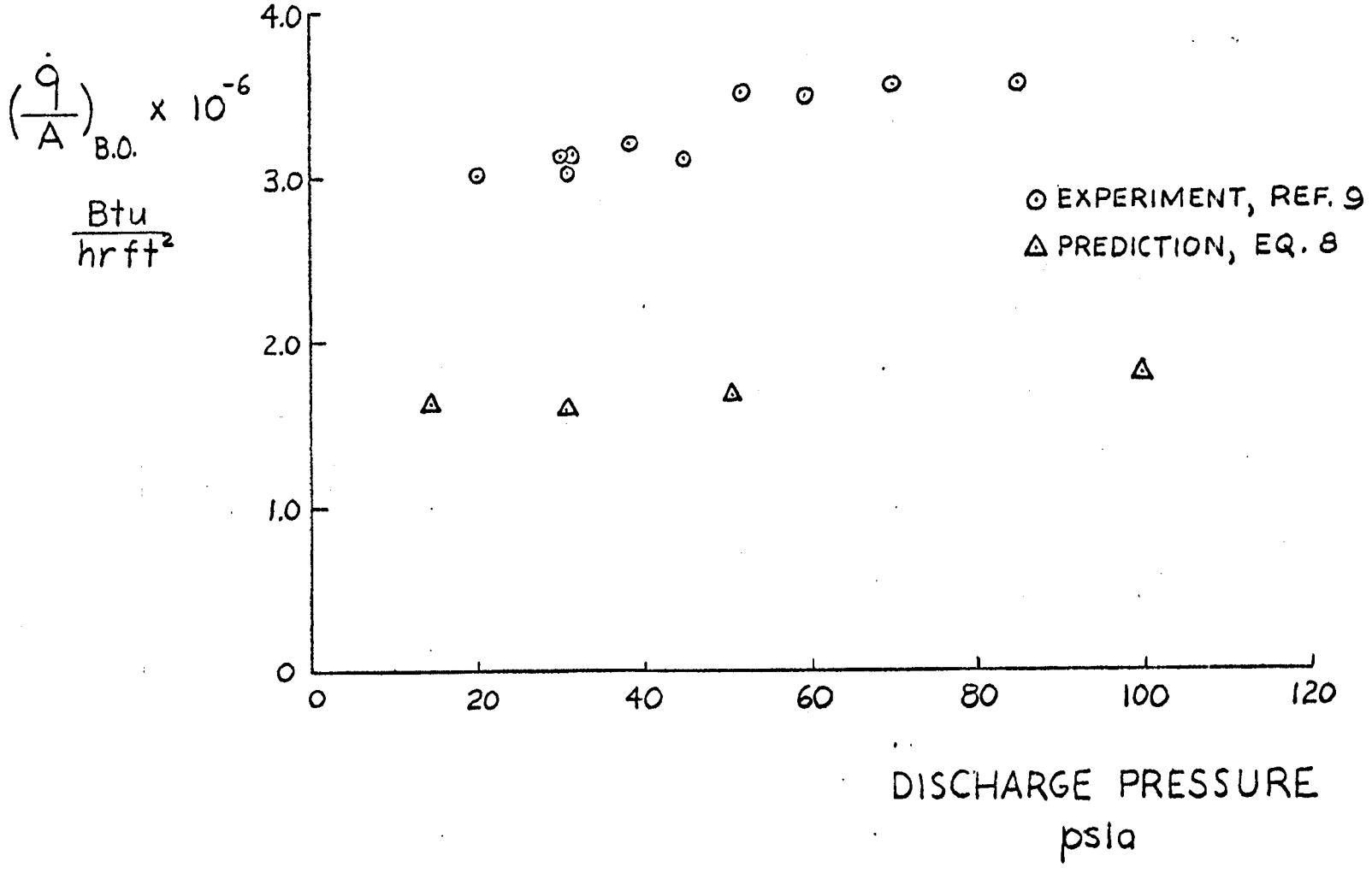

V. Experimental Apparatus

Constrictors with several different coolant passage configurations were built and tested in the apparatus shown in Fig. 13. A direct current arc was initiated between the carbon electrodes through three test constrictors. Distilled water was circulated through each constrictor, and the flow rate through the center constrictor was metered with a rotameter. The energy input to the center constrictor was determined by an energy balance on its coolant flow, utilizing upstream and downstream thermocouples on the center constrictor flow lines. This coolant flow temperature difference was recorded on a CEC recording oscillograph along with the arc current.

Boron nitride was used for the insulating wafers on both sides of all three constrictors. The outermost wafers were replaced after each run, and these plus the larger boron nitride end pieces, served to shield the constrictors from the anode and cathode heating. It is felt that this shielding was successful in reducing end effects since some runs were taken with only the test constrictor between the two shields, and the results of these runs compared favorably with those obtained with three constrictors.

The constrictor configurations tested are shown in Figures 14 through 17. Ten constrictors of each type were fabricated. The radius ration, r_o/r_i, on the two port and four port configuration is 1.4. On the eight port configuration, radius ratios of both 1.4 and 1.6 were tested. In addition, some older constrictors of both two port and four port designs, but with a radius ratio of 2.75, were tested. These older constrictors were electron beam fabricated rather than silver brazed. All of the test constrictors had plasma hole diameters of 0.25 inches.

FIGURE 13

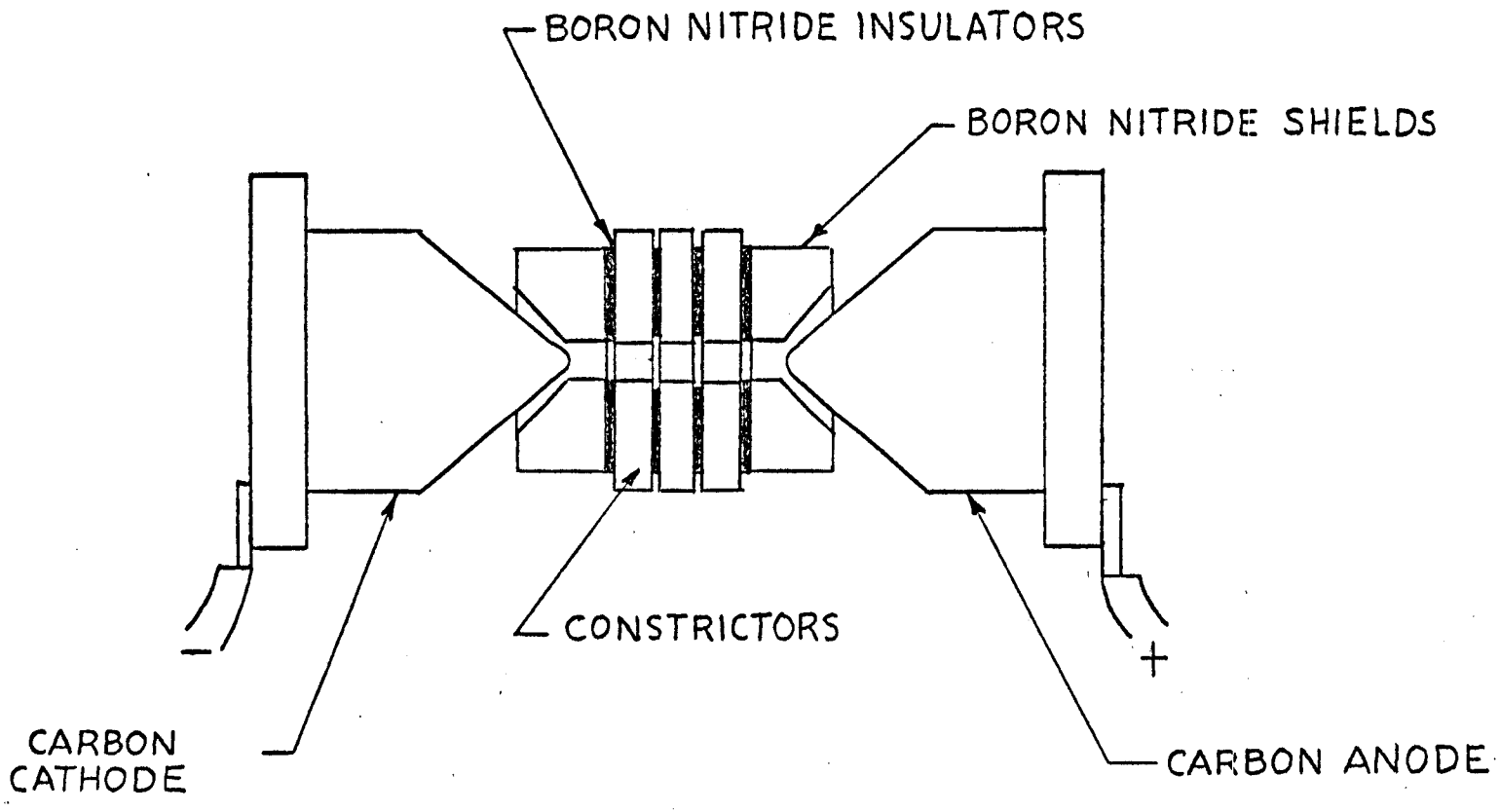

EXPERIMENTAL APPARATUS

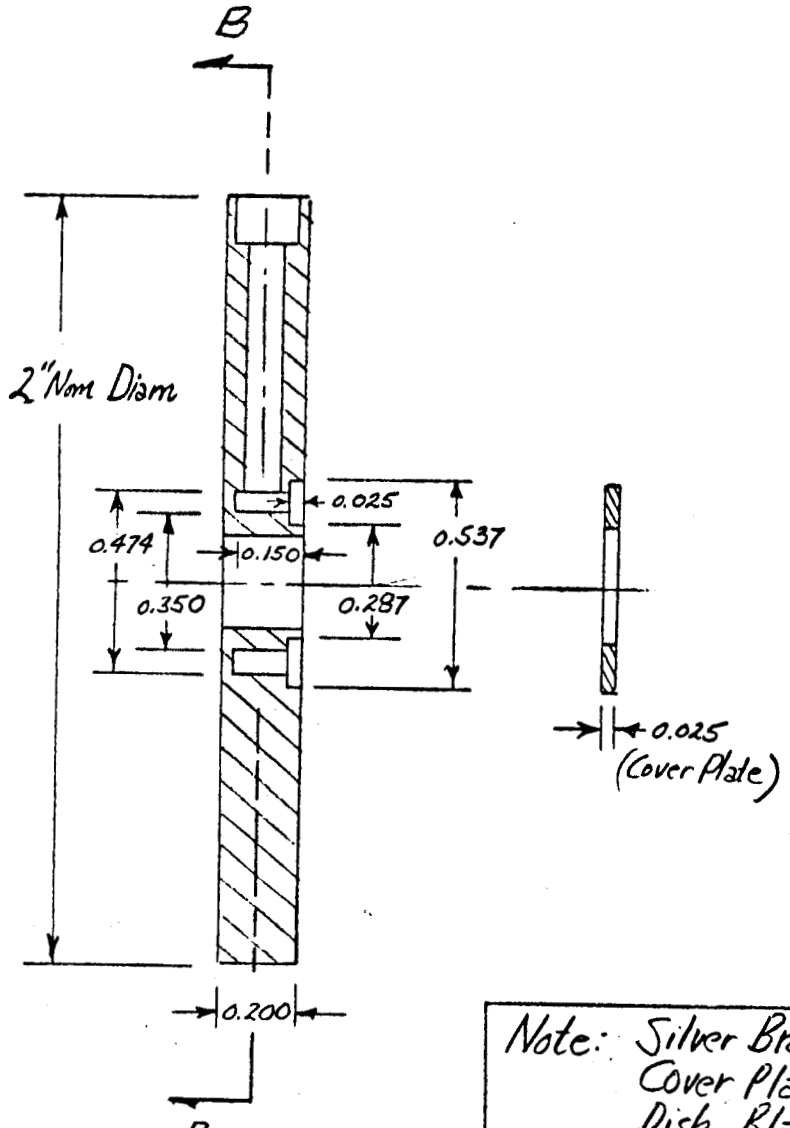

SECTION A-A

Note: Silver Braze Cover Plate to Disk Blank.

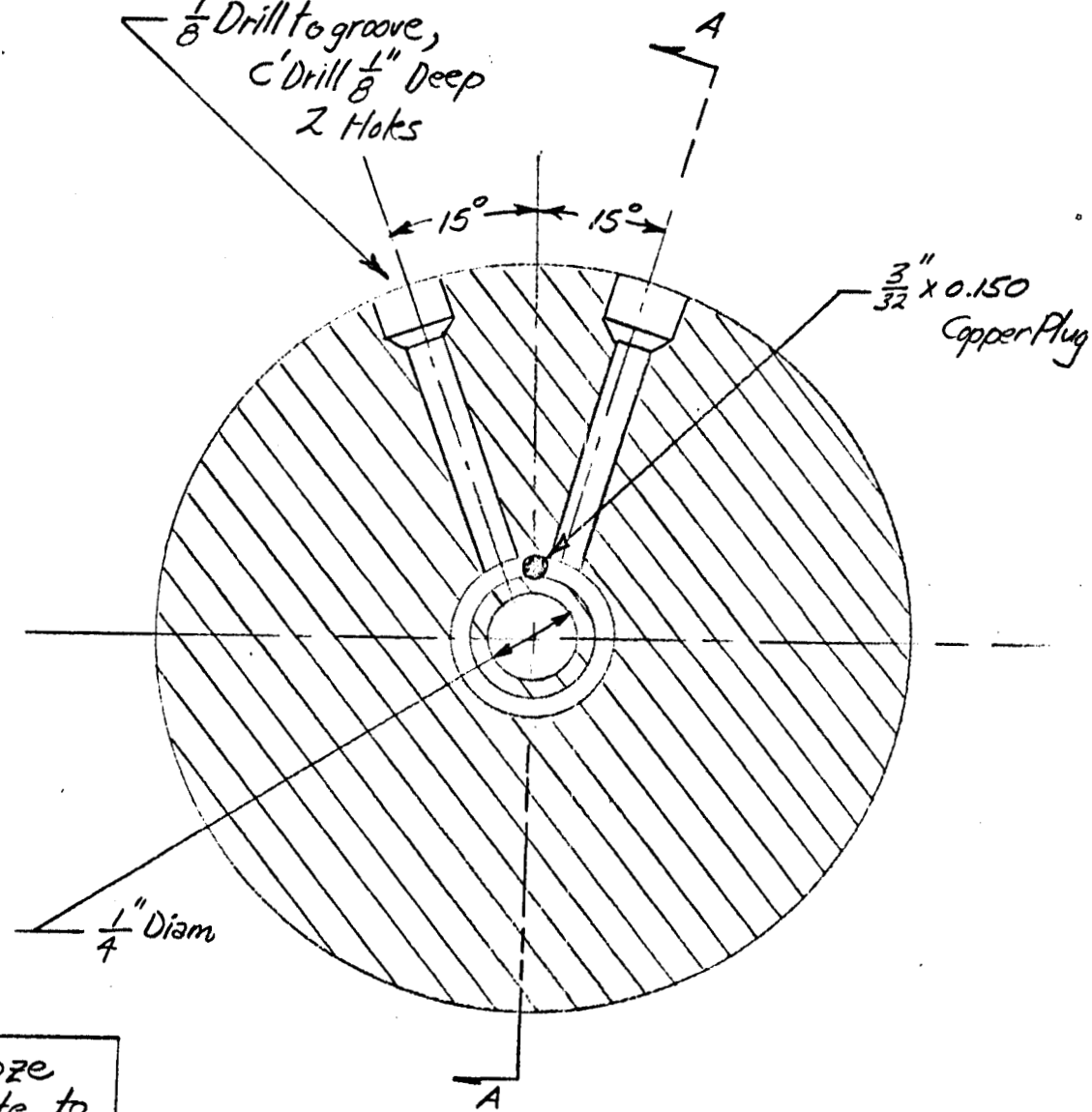

SECTION B-B

CONSTRICTOR DISK 1.4	
10 REQ'D	O.F.H.C. COPPER
D.E. Metzger	X2696
Bldg N-229-2	
JO R 2607	

FIGURE 14

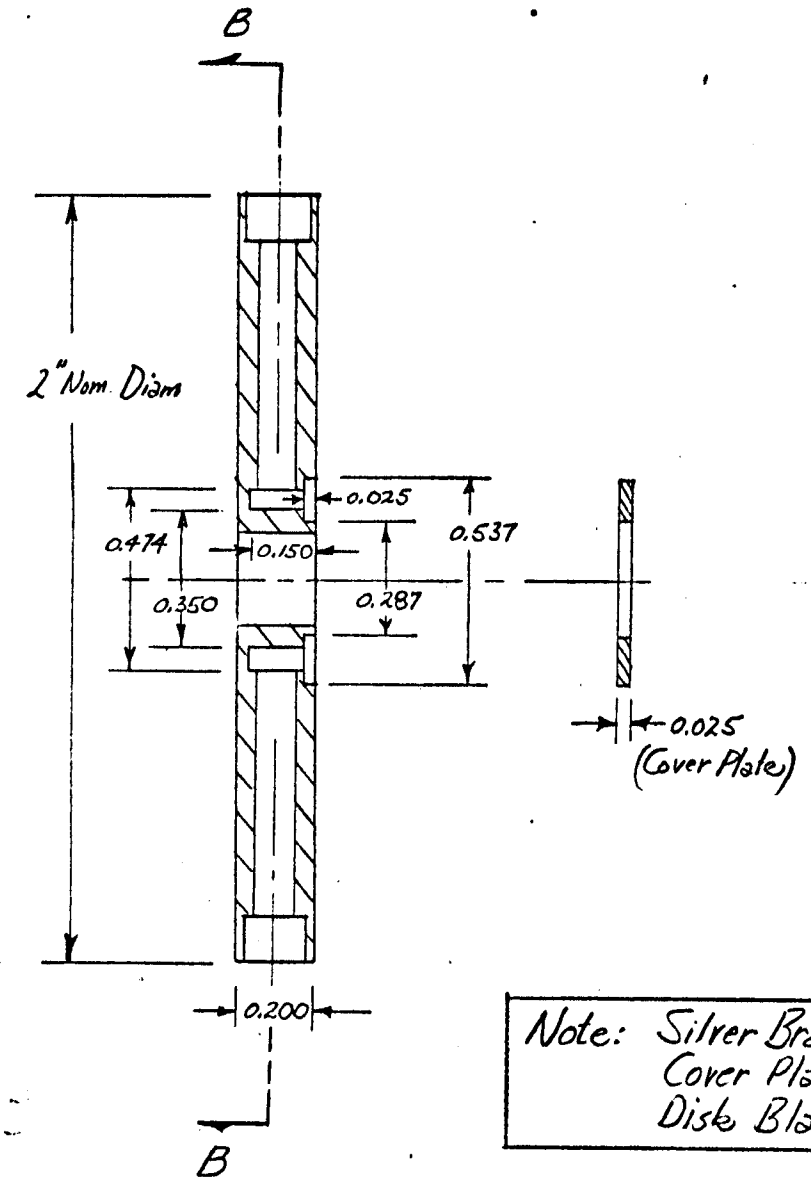

SECTION A-A

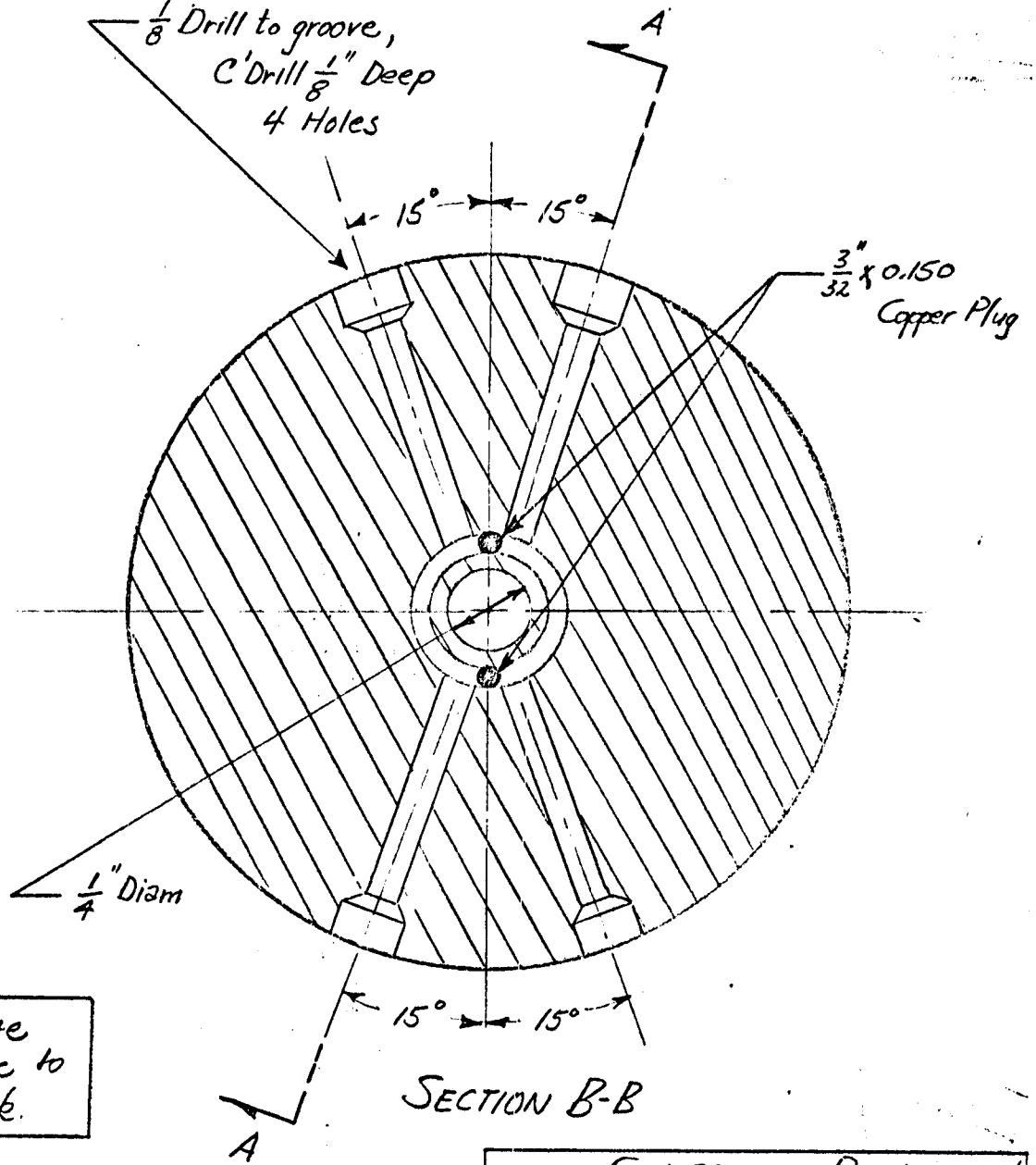

SECTION B-B

Note: Silver Braze Cover Plate to Disk Blank.

CONSTRICTOR DISK 1.4	
10 REQ'D	O.F.H.C. COPPER
D.E. Metzger	X2696
Bldg N-229-2	
J.O. R 2607	

FIGURE 15

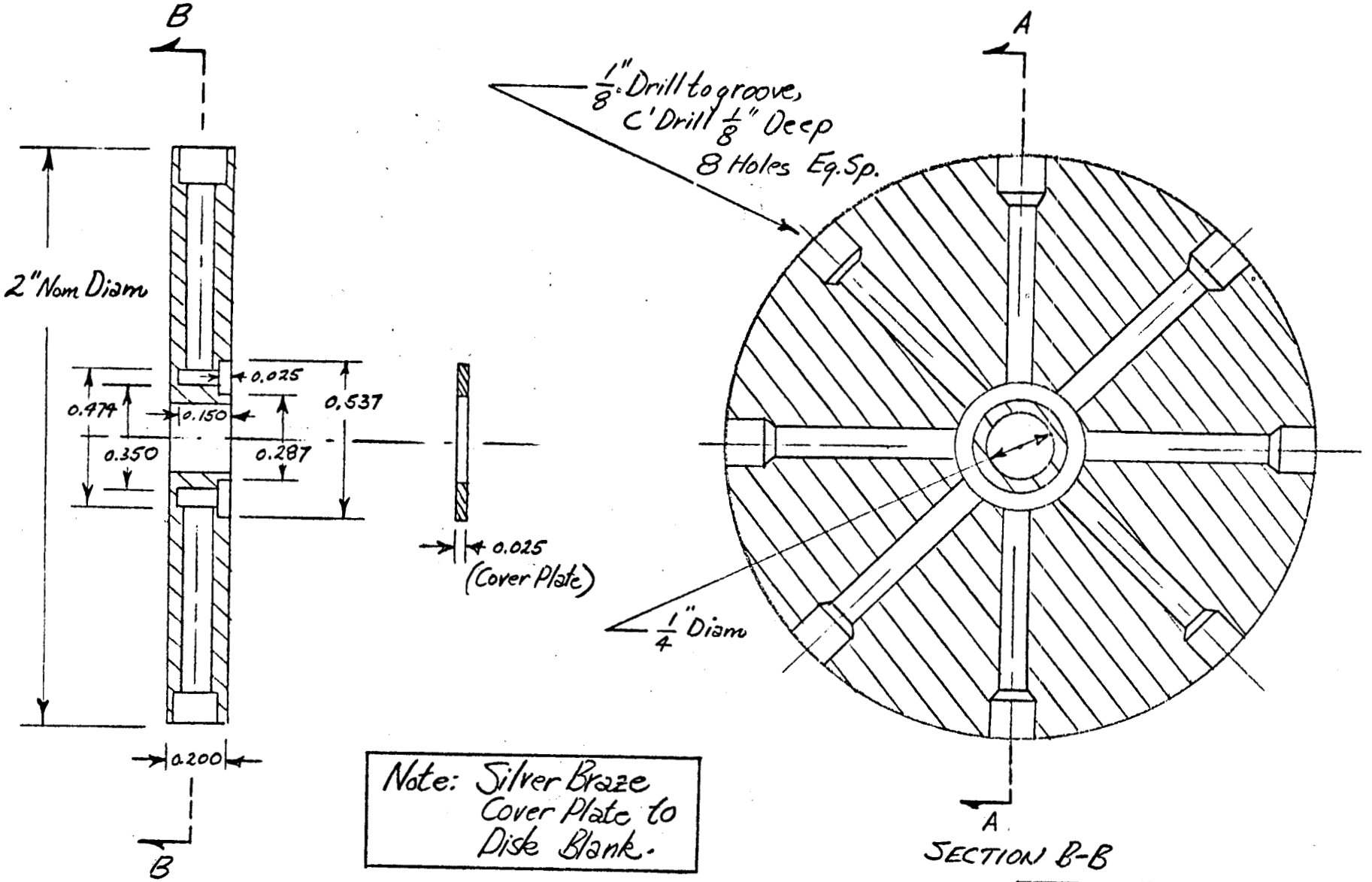

Note: Silver Braze Cover Plate to Disk Blank.

CONSTRICTOR DISK	1.4
10 REQ'D	O.F.H.C. COPPER
D.E. Metzger	X 2696
Bldg N-229-2	
JO R 2607	

FIGURE 16

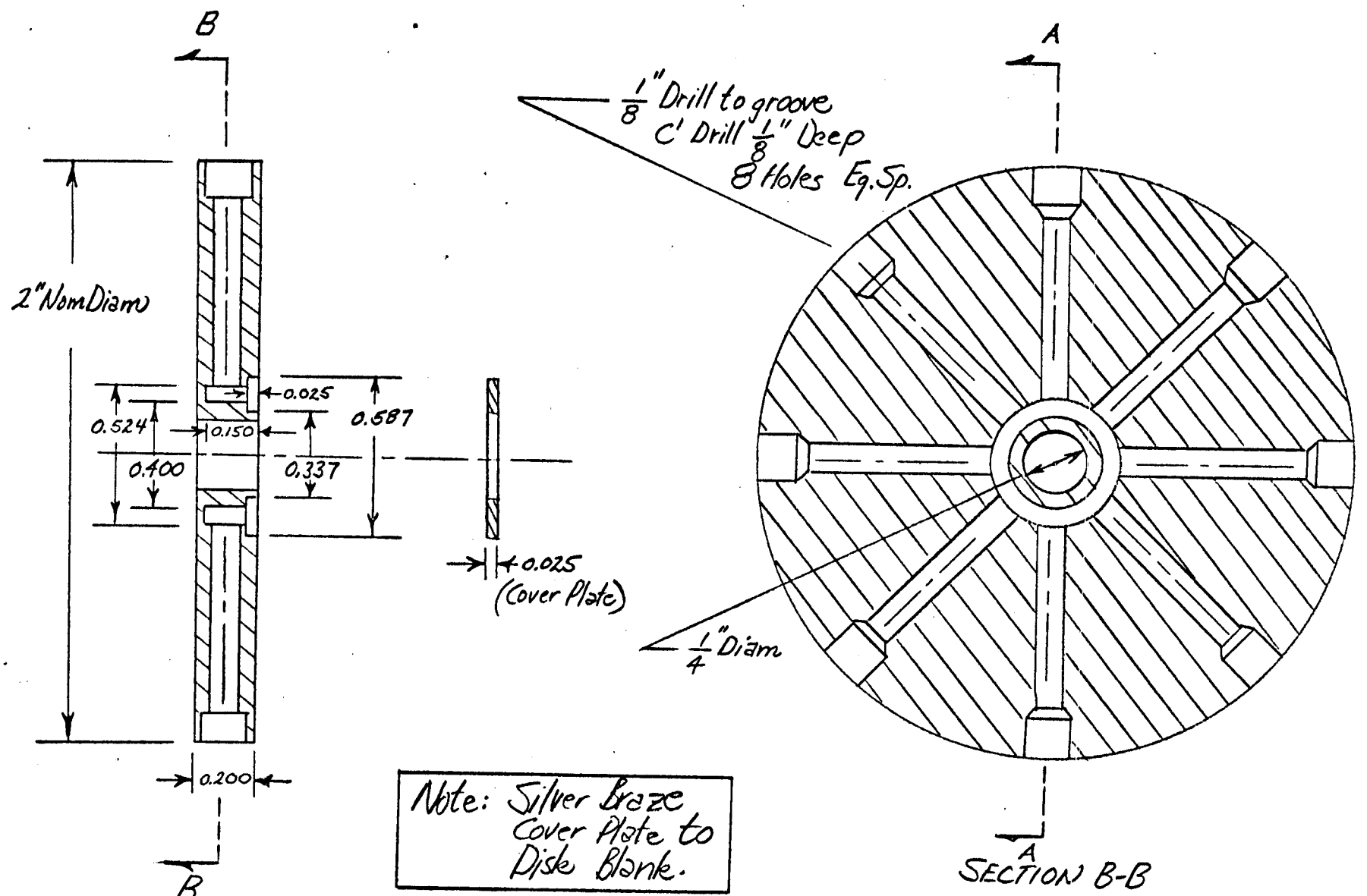

Note: Silver Braze Cover Plate to Disk Blank.

CONSTRICTOR DISK	1.6
10 REQ'D	O.F.H.C. COPPER
D.F. Metzger	X2696
Bldg N-229-2	
JO R 2607	

FIGURE 17

VI. Experimental Results

Melting Failures. In testing each constrictor configuration, successive runs were made with increasing arc currents until rupture of the coolant passage occurred. The time required to achieve steady state, as indicated by the recorder traces, was approximately two seconds. A typical recorder trace is shown in Figure 18.

Many of the test sequences with the electron beam welded constrictors were terminated prior to a true failure by the appearance of stress leaks at the weld. Some of the silver brazed constrictors also developed leaks around the braze, but these were found to be much more reliable than the beam welded disks.

For the 2.75 radius ratio constrictors with good welds, the pattern of failure was as follows. First, after a run at a certain current level, the dismantled constrictors exhibited melting at the edges of the plasma hole. In most cases, there was mainly rounding of the edges of the hole, but in some cases there was a noticeable enlargement of the hole diameter. This first stage of melting took place without causing any coolant passage leaks; however, subsequent runs with slightly higher arc currents always resulted in a complete failure of the coolant passage. For both the two and four port 2.75 radius ratio constrictors, the first signs of melting occurred at plasma side heat fluxes of from 3500 to 4000 Btu/(ft^2sec). This value is consistent with Figure 3, which predicts premature melting for these constrictors.

A possible explanation for the subsequent failure of these constrictors is that the liquid copper shorts across the boron nitride separating the constrictors, resulting in attachment of the arc to the constrictors and increased local heating rates at the attachment points.

Burnout Failures. The failure pattern observed in the test sequences for the 1.4 and 1.6 radius ratio constrictors was quite different than that followed by the larger radius ratio disks. Failure in these tests occurred before steady state was reached, but at a flux level higher than that reached in the preceding run at steady state. No local melting was noted in the run immediately preceding the failure. This conforms to the pattern that would be expected for a burnout failure. The failure in all cases was accompanied by a distinct "pop" sound,

which could be characteristic of burnout in this situation. The failure in these tests was generally very complete, with large portions of the coolant passage wall completely destroyed.

In the two and four port constrictors, the flow turning and accelerations are such that any vapor formed which remains in the flow would be forced to the heated side of the passage by buoyant forces. This would enhance the possibility of the vapor coalescing into a film, triggering burnout. This tendency is overcome by the eight port design which essentially reverses the turning direction. Moreover, this design takes advantage of the high convective heat transfer coefficients normally associated with flow impingement normal to a surface.

The test results indicate burnout fluxes from 5,000 to 6,000 Btu/(ft^2sec) for the two port design, around 6,400 Btu/(ft^2sec) for the four port design, and between 7,000 and 8,000 Btu/(ft^2sec) for the eight port design.

The failure results for test sequences not spoiled by stress leaks are summarized in Table I. For all the runs the supply pressure was approximately 100 psia; the discharge pressure approximately 30 psia.

TABLE I - EXPERIMENTAL RESULTS

Run No.	No. of Ports	r_o/r_i	$(\dot{q}/A)_i$ [a]	$(\dot{q}/A)_o$ [a]	Failure Type
12	2	2.75	10,000	3,630	b
18	2	2.75	9,650	3,510	b
22	2	2.75	10,300	3,700	b
26	4	2.75	10,800	3,930	b
29	4	2.75	10,300	3,690	b
39	2	1.40	7,450	5,320	c
48	2	1.40	8,300	5,930	c
43	4	1.40	9,050	6,450	c
45	4	1.40	8,900	6,360	c
34	8	1.60	12,000	7,500	c
37	8	1.60	11,500	7,200	c
51	8	1.60	12,200	7,630	c
40	8	1.40	10,600	7,580	c
53	8	1.40	11,200	8,000	c

a Btu/(ft^2sec)

b Melting, further increases in heat flux result in failure

c Apparent burnout

FIGURE 18
TYPICAL RECORDER TRACE

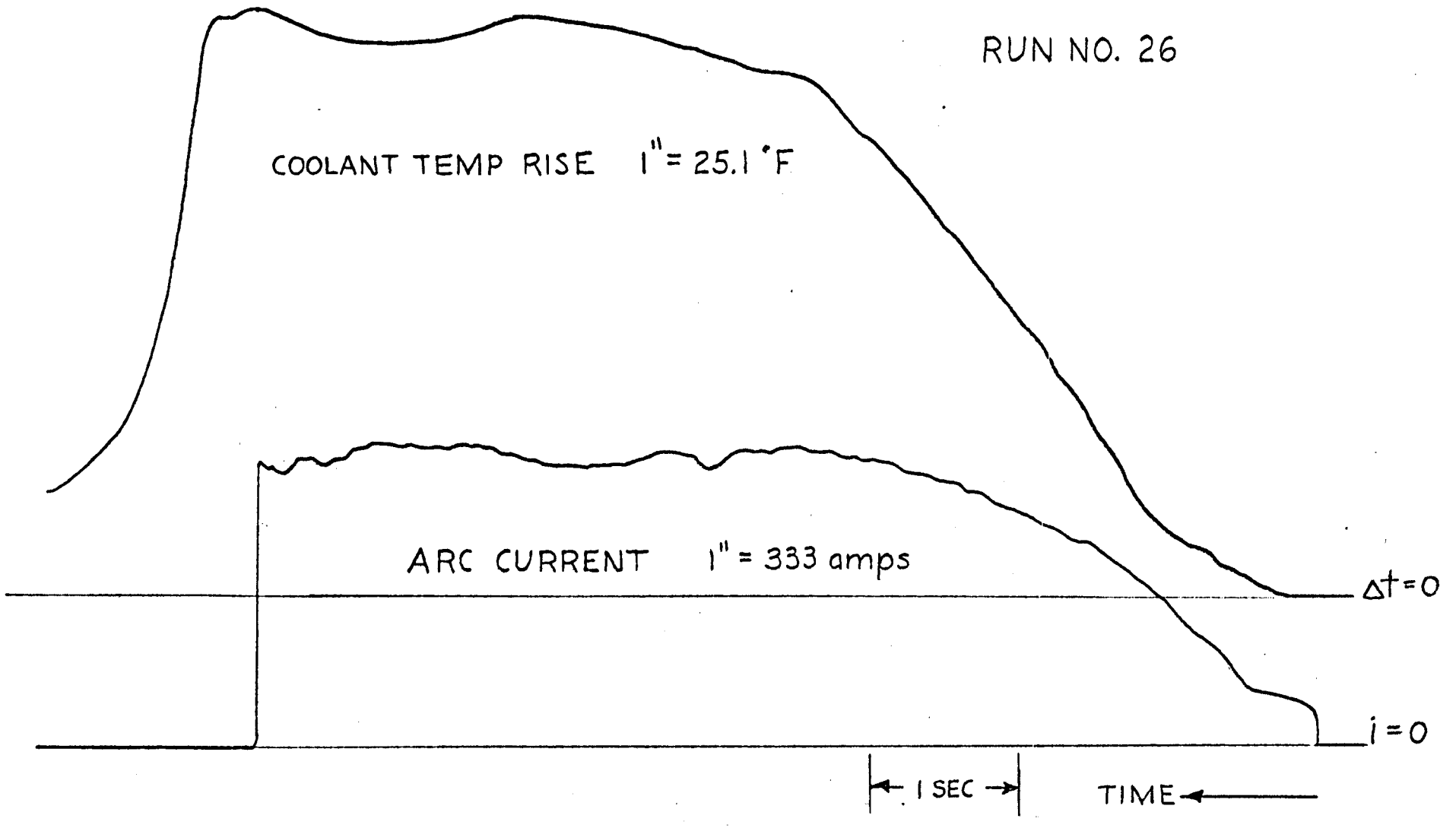

VII. Discussion

The eight port constrictor configuration was designed and tested with the thought that the reverse turning of the flow would result in a delaying of transition boiling and an increase in the critical heat flux. The present test results appear to support this argument; however, it may be that the higher burnout flux is due more to higher non-boiling convection coefficients than to any enhancement of the boiling behavior. It can be observed in a comparison of Figures 7 and 11 that the non-boiling convective contribution to the burnout heat flux is a large percentage of the total flux even at low supply pressures, and accounts for an even larger amount at higher supply pressures. As a result, increases in the non-boiling convective coefficient result in significantly higher burnout fluxes.

The highest burnout fluxes observed in the present tests are approximately four times higher than those predicted by Figure 11; however, it is not inconceivable that the convective coefficients are four times higher than those calculated by the Colburn Equation. The developing, impinging flow, together with heating on only one wall and a strong secondary flow pattern, are factors which would tend to increase the average passage heat transfer coefficient. In addition, it should be noted that the reported heat fluxes are based on the heated side area only. Some heating does occur on the sides of the passage, and the effective coolant side fluxes may be only 1/2 to 2/3 the reported values.

Without specific non-boiling heat transfer correlations for the constrictor geometry and boundary conditions, it is impossible to determine the relative magnitude of the burnout flux and the flux at incipient boiling. If the boiling contribution is small, then constrictors should be designed to operate below incipient boiling, where problems such as flow oscillation and flow excursion do not occur.

The compressibility of the flow system can lead to these instabilities when boiling takes place inside the flow passage. The instabilities result in premature burnout soon after boiling starts. The problem can be solved by throttling the flow immediately upstream of the heated section, but this

reduces the system head and the convective coefficient. In the present tests, no throttling was done upstream of the constrictors, and the burnout observed could be the result of flow oscillation.

With the present test data, and the trends predicted by Figure 11, it seems possible that coolant side fluxes up to 2-1/2 times the present values, or 18,000 Btu/(sec ft^2) can be achieved with a 1000 psia supply pressure.